Fluorescence Color Modulation by Intramolecular and Intermolecular $\pi-\pi$ Interactions in a Helical Zinc(II) Complex

Shin Mizukami,*,† Hirohiko Houjou,‡ Kenta Sugaya,† Emiko Koyama,† Hideo Tokuhisa,† Takeshi Sasaki,† and Masatoshi Kanesato*,†

Nanoarchitectonics Research Center, National Institute of Advanced Industrial Science and Technology, Tsukuba Central 4, 1-1-1 Higashi, Tsukuba, Ibaraki 305-8562, Japan, and Institute of Industrial Science, The University of Tokyo, 4-6-1 Komaba Meguro-ku, Tokyo 153-8505, Japan

Received February 19, 2004. Revised Manuscript Received October 22, 2004

When a fluorescent compound shows unique optical properties, an elucidation of the mechanism may lead to an important development of novel sensing strategies. A helical 3,3′-di-*tert*-butylsalen−zinc(II) complex, $[Zn_2\mathbf{L^1}_2]$, has a red-shifted fluorescence as compared to that of $[Zn\mathbf{L^2}_2]$, a half-structured mononuclear complex of $[Zn_2\mathbf{L^1}_2]$; in addition, $[Zn_2\mathbf{L^1}_2]$ exhibits a fluorescence color change from green to light blue under external stimulations. We investigated the origins of these phenomena by spectroscopy, fluorescence lifetime measurement, fluorescence microscopy, X-ray powder diffraction, and X-ray single-crystal analysis. From the experimental data, we concluded that intramolecular and intermolecular $\pi-\pi$ interactions are critical elements that determine the shifts of the fluorescence to a longer wavelength.

Introduction

Fluorescent compounds are very important materials. When they are fluorescent in solution, they can be leading compounds for the development of fluorescent sensors.[1] When they are fluorescent in the solid state, they may be good candidates for gas sensors[2,3] or electroluminescent materials.[4−6] The fluorescence of the salicylideneamine complexes with several elements is very strong;[7−9] in particular, the salicylideneamine−zinc(II) complexes exhibit electroluminescence as well as photoluminescence.[10,11] Recently, we reported the synthesis and the structure of a zinc(II)−salen helical complex $[Zn_2\mathbf{L^1}_2]$ (Figures 1 and 2a).[12] This complex, the first double helical zinc(II) complex with a salen ligand, displayed a strong fluorescence both in solution and in the solid state. Interestingly, the photoluminescence spectrum of $[Zn_2\mathbf{L^1}_2]$ was quite different from that of the half-structured complex $[Zn\mathbf{L^2}_2]$ (Figures 1, 2b). Moreover, when the crystals of $[Zn_2\mathbf{L^1}_2]$ were crushed to a powder, the photoluminescence shifted to a shorter wavelength, and, after the crystal of $[Zn_2\mathbf{L^1}_2]$ reacted with certain organic vapors, it demonstrated vapochromism.

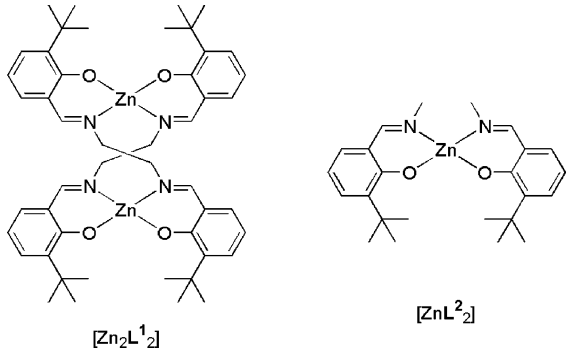

Figure 1. Chemical structures of $[Zn_2\mathbf{L^1}_2]$ and $[Zn\mathbf{L^2}_2]$.

Currently, many researchers are focusing on the $\pi-\pi$ stacking interactions of aromatic rings, phenomena universally observed in nature. Evidently, London dispersion interactions are the major source of this interaction,[13] which then affects the electronic states of stacking aromatic groups. Although $\pi-\pi$ stacking quenches most fluorescent compounds in solution, some compounds still fluoresce and shift their fluorescence to a longer wavelength.[14,15] In the solid state, the packing structures affect the solid luminescence of some compounds.[16−18] Recent studies involving tris(8-hydroxyquinoline)-aluminum(III) (Alq_3), which is one of the

* Corresponding author. Tel.: +81-29-861-3022. Fax: +81-29-861-3029. E-mail: m.kanesato@aist.go.jp.
† National Institute of Advanced Industrial Science and Technology.
‡ The University of Tokyo.

(1) deSilva, A. P.; Gunaratne, H. Q. N.; Gunnlaugsson, T.; Huxley, A. J. M.; McCoy, C. P.; Rademacher, J. T.; Rice, T. E. *Chem. Rev.* **1997**, *97*, 1515−1566.
(2) Dickinson, T. A.; White, J.; Kauer, J. S.; Walt, D. R. *Nature* **1996**, *382*, 697−700.
(3) Li, D.; Mills, C. A.; Cooper, J. M. *Sens. Actuators, B* **2003**, *92*, 73−80.
(4) Tang, C. W.; Vanslyke, S. A. *Appl. Phys. Lett.* **1987**, *51*, 913−915.
(5) Chen, C. H.; Shi, J. M. *Coord. Chem. Rev.* **1998**, *171*, 161−174.
(6) Sapochak, L. S.; Benincasa, F. E.; Schofield, R. S.; Baker, J. L.; Riccio, K. K. C.; Fogarty, D.; Kohlmann, H.; Ferris, K. F.; Burrows, P. E. *J. Am. Chem. Soc.* **2002**, *124*, 6119−6125.
(7) Freeman, D. C.; White, C. E. *J. Am. Chem. Soc.* **1956**, *78*, 2678−2682.
(8) White, C. E.; Cuttitta, F. *Anal. Chem.* **1959**, *31*, 2083−2087.
(9) Dagnall, R. M.; Smith, R.; West, T. S. *J. Chem. Soc. A* **1966**, 1595−1598.
(10) Hamada, Y.; Sano, T.; Fujita, M.; Fujii, T.; Nishio, Y.; Shibata, K. *Jpn. J. Appl. Phys., Part 2* **1993**, *32*, L511−L513.
(11) Sano, T.; Nishio, Y.; Hamada, Y.; Takahashi, H.; Usuki, T.; Shibata, K. *J. Mater. Chem.* **2000**, *10*, 157−161.
(12) Mizukami, S.; Houjou, H.; Nagawa, Y.; Kanesato, M. *Chem. Commun.* **2003**, 1148−1149.
(13) Meyer, E. A.; Castellano, R. K.; Diederich, F. M. *Angew. Chem., Int. Ed.* **2003**, *42*, 1211−1250.
(14) Nishizawa, S.; Kato, Y.; Teramae, N. *J. Am. Chem. Soc.* **1999**, *121*, 9463−9464.
(15) Wang, W.; Han, J. J.; Wang, L. Q.; Li, L. S.; Shaw, W. J.; Li, A. D. Q. *Nano Lett.* **2003**, *3*, 455−458.

10.1021/cm049744s CCC: $30.25
Published on Web 12/13/2004

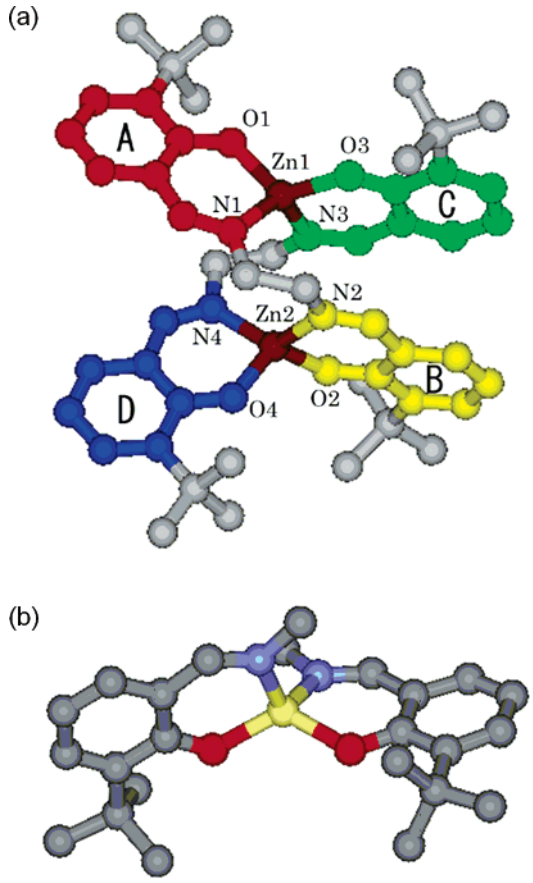

Figure 2. Crystal structures of (a) $[Zn_2\mathbf{L}^1_2]$ and (b) $[Zn\mathbf{L}^2_2]$.

most successful compounds used in organic light-emitting diodes (OLEDs), agree that the form of the molecular packing affects the optical properties.[19−22] In every case, investigators noted the existence of $\pi-\pi$ stacking of the chromophores.

In this paper, we report the optical properties and the fluorescence changes of $[Zn_2\mathbf{L}^1_2]$ obtained by external stimulations and discuss the mechanism from the viewpoint of intramolecular and intermolecular $\pi-\pi$ interactions. Understanding the mechanism of such luminochromism may pioneer a new methodology of fluorescence sensing.

Experimental Section

General Remarks. We recorded proton and carbon nuclear magnetic resonance (^{1}H and ^{13}C NMR) spectra on Bruker AVANCE500 spectrometers; to record the electrospray ionization mass spectra (ESI-MS), we used a Waters 2690 separations module, a micromass ZMD, and a Waters 996 photodiode array detector.

Materials. We synthesized the dinulclear zinc(II)−salen complex $[Zn_2\mathbf{L}^1_2]$ and the half-structured mononuclear complex $[Zn\mathbf{L}^2_2]$ as described previously.[12] To obtain other single crystals, we dissolved the $[Zn_2\mathbf{L}^1_2]$ in tetrahydrofuran (THF) and diluted it with acetonitrile (THF/acetonitrile = 1/9 (v/v)). This solution was allowed to slowly evaporated until some single green fluorescent crystals appeared, which were confirmed to be $[Zn_2\mathbf{L}^1_2]$·THF by X-ray crystallography. When zinc(II) acetate dihydrate, 3-*tert*-butylsalicylaldehyde, and ethylenediamine (1:2:1) were mixed without stirring in absolute methanol at room temperature, precipitates appeared after several days. Although most of the solids were nonfluorescent, some crystals fluoresced blue; X-ray crystallography confirmed that these were $[Zn\mathbf{L}^2_2]$·MeOH.

Absorption and Emission Spectra. We measured the absorption spectra of $[Zn_2\mathbf{L}^1_2]$ (10 μM) and $[Zn\mathbf{L}^2_2]$ (20 μM) at 25 °C, using a spectrophotometer (JASCO, V-750 UV/VIS/NIR), and both the solution (1 μM in acetonitrile) and the solid fluorescence spectra at the same temperature with a spectrofluorometer (JASCO, FP-750). The fluorescence quantum yields were measured according to the reported method.[23] Quinine sulfate in 0.50 M aqueous H_2SO_4 was used as a standard compound.

Fluorescence Lifetime. The fluorescence lifetimes were measured with a fluorescence lifetime spectrometer (Photon Technology International, PTI-3000). All compounds were excited at 337 nm.

Fluorescence Microscopy. All samples were observed with a fluorescence microscope (OLYMPUS, BX60) with U-MWU filter units (DM400/BP330-385/BA420) using a mercury laser (OLYMPUS, U-ULS-100HG) for the excitation. The fluorescence images were captured by a CCD camera (OLYMPUS, CS-580).

X-ray Powder Diffraction Analysis. X-ray powder diffraction data were obtained with graphite-monochromated Cu Kα radiation (λ = 1.5406 Å) on an X-ray powder diffractometer (Rigaku RAD-C).

X-ray Single-Crystal Analysis. The crystal data for all compounds were recorded on a Rigaku RAXIS-RAPID imaging plate diffractometer with graphite-monochromated Mo Kα radiation (λ = 0.7107 Å) at −80 °C in the $\omega-2\theta$ mode. All non-hydrogen atoms were refined anisotropically. The structures were solved by the direct method and expanded using Fourier techniques. An absorption correction was carried out for all data. All of the structural analysis and adjustments used the CrystalStructure crystallographic software package (Rigaku Corp.).

Results and Discussion

I. Fluorescence Color Modulation by Intramolecular $\pi-\pi$ Interactions of Helical Structure. In our previous paper,[12] we noted that the fluorescence colors of dinuclear $[Zn_2\mathbf{L}^1_2]$ (green) were different from those of mononuclear $[Zn\mathbf{L}^2_2]$ (blue), although the chromophores of $[Zn_2\mathbf{L}^1_2]$ and $[Zn\mathbf{L}^2_2]$ were almost identical. The absorption spectra of $[Zn_2\mathbf{L}^1_2]$ and $[Zn\mathbf{L}^2_2]$ in acetonitrile are shown in Figure 3a; the absorption maximum wavelengths (λ_{abs}) are 382 nm ($[Zn_2\mathbf{L}^1_2]$) and 370 nm ($[Zn\mathbf{L}^2_2]$). The molar extinction coefficients ϵ of the two complexes were 2.06×10^4 and 1.22×10^4 M^{-1} cm^{-1}, respectively. The averaged molar extinction coefficient for the chromophoric unit, in other words, salicylideneamine, was 5.15×10^3 M^{-1} cm^{-1} for $[Zn_2\mathbf{L}^1_2]$ and 6.10×10^3 M^{-1} cm^{-1} for $[Zn\mathbf{L}^2_2]$. Figure 3b presents the emission spectra in acetonitrile. As the excitation wavelengths, we chose the maximum absorption wavelengths

(16) Yoshida, K.; Miyazaki, H.; Miura, Y.; Ooyama, Y.; Watanabe, S. *Chem. Lett.* **1999**, 837−838.
(17) Lu, W.; Chan, M. C. W.; Cheung, K. K.; Che, C. M. *Organometallics* **2001**, *20*, 2477−2486.
(18) Yoshida, K.; Ooyama, Y.; Tanikawa, S.; Watanabe, S. *J. Chem. Soc., Perkin Trans. 2* **2002**, 708−714.
(19) Brinkmann, M.; Gadret, G.; Muccini, M.; Taliani, C.; Masciocchi, N.; Sironi, A. *J. Am. Chem. Soc.* **2000**, *122*, 5147−5157.
(20) Muccini, M.; Brinkmann, M.; Gadret, G.; Taliani, C.; Masciocchi, N.; Sironi, A. *Synth. Met.* **2001**, *122*, 31−35.
(21) Braun, M.; Gmeiner, J.; Tzolov, M.; Coelle, M.; Meyer, F. D.; Milius, W.; Hillebrecht, H.; Wendland, O.; von Schutz, J. U.; Brutting, W. *J. Chem. Phys.* **2001**, *114*, 9625−9632.
(22) Colle, M.; Dinnebier, R. E.; Brutting, W. *Chem. Commun.* **2002**, 2908−2909.
(23) Demas, J. N.; Crosby, G. A. *J. Phys. Chem.* **1971**, *75*, 991−1024.

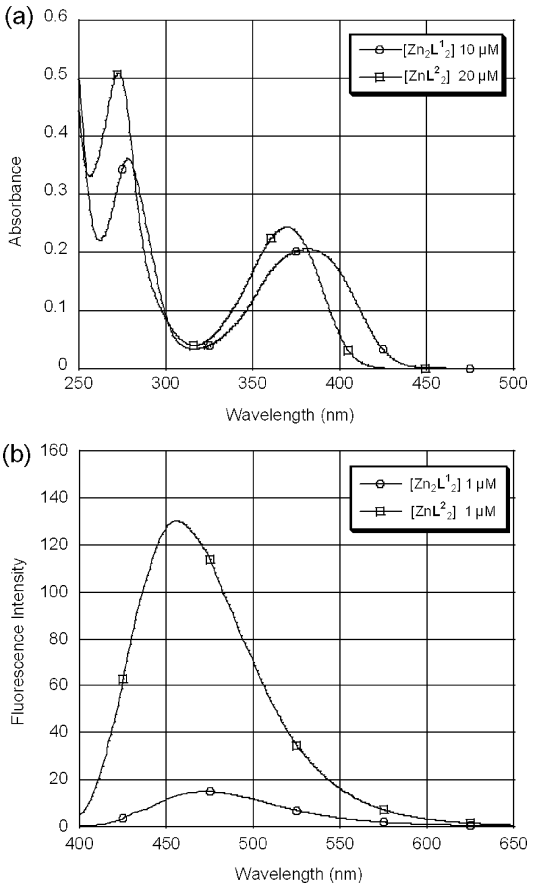

Figure 3. (a) Absorption and (b) emission spectra of $[Zn_2\mathbf{L^1}_2]$ and $[Zn\mathbf{L^2}_2]$ in acetonitrile solution.

Table 1. Fluorescence Quantum Yields and Liftimes of $[Zn_2\mathbf{L^1}_2]$ and $[Zn\mathbf{L^2}_2]$[a]

complex	Φ	τ (ns)
$[Zn_2\mathbf{L^1}_2]$	0.017[b]	1.21,[d] 1.04,[e] 3.17[f]
$[Zn\mathbf{L^2}_2]$	0.24[c]	5.24,[d] 6.16[e]

[a] All samples were excited at 337 nm. [b] 1.0×10^{-5} M acetonitrile solution. [c] 2.0×10^{-5} M acetonitrile solution. [d] 1.0×10^{-4} M acetonitrile solution. [e] Single crystal. [f] Crushed crystal.

(λ_{abs}); the emission maximum wavelengths are 473 nm ($[Zn_2\mathbf{L^1}_2]$) and 456 nm ($[Zn\mathbf{L^2}_2]$). Both the absorption and the emission spectra of $[Zn_2\mathbf{L^1}_2]$ were red-shifted as compared to those of $[Zn\mathbf{L^2}_2]$. The intensity of the $[Zn_2\mathbf{L^1}_2]$ fluorescence was much lower than that of $[Zn\mathbf{L^2}_2]$, although $[Zn_2\mathbf{L^1}_2]$ has twice as many chromophores as $[Zn\mathbf{L^2}_2]$. Their fluorescence quantum yields (Φ) were 0.017 ($[Zn_2\mathbf{L^1}_2]$) and 0.24 ($[Zn\mathbf{L^2}_2]$) (Table 1).

To investigate the differences between these compounds, we next carried out a comparative analysis of their molecular structures. The crystal structures of $[Zn_2\mathbf{L^1}_2]$ and $[Zn\mathbf{L^2}_2]$ obtained from an X-ray crystal structure analysis, the results of which we briefly reported previously,[12] are shown in Figure 2a and b. Tables 2 and 3 list the crystal and experimental data and selected bond lengths and angles of the complexes. The crystallographic data revealed no remarkable differences in the bond lengths and angles in the chromophoric units. The largest difference between $[Zn_2\mathbf{L^1}_2]$ and $[Zn\mathbf{L^2}_2]$ is that $[Zn_2\mathbf{L^1}_2]$ is a helical complex. In $[Zn_2\mathbf{L^1}_2]$, every chromophoric unit is parallel to one of the others, but in $[Zn\mathbf{L^2}_2]$, the two chromophores of $[Zn\mathbf{L^2}_2]$ are located almost orthogonally. In Figure 2a, we define the chromophoric heterocycles as A (red), B (yellow), C (green), and D (blue). They form two pairs with an intramolecular $\pi-\pi$ stacking, A−D and B−C. The distances between N1−N4 and N2−N3, 3.284 and 3.217 Å, are almost equivalent to the interplanar distances of chromophore pairs A−D and B−C.

The crystal analysis strongly suggests the existence of an intramolecular $\pi-\pi$ interaction in $[Zn_2\mathbf{L^1}_2]$; such an intramolecular $\pi-\pi$ interaction could account for the results of the absorption and emission spectra in solution.

Fluorescence lifetime experiment also supports the existence of the interaction. In acetonitrile solution, the fluorescence lifetimes of $[Zn_2\mathbf{L^1}_2]$ and $[Zn\mathbf{L^2}_2]$ were 1.21 and 5.24 ns, respectively (Table 1). These data imply that the excited singlet state of $[Zn_2\mathbf{L^1}_2]$ became short-lived by the intramolecular $\pi-\pi$ interaction.

Thus, we conclude that its different spectral features of $[Zn_2\mathbf{L^1}_2]$ originate in the intramolecular $\pi-\pi$ interaction in its unique helical structure. This result suggests that helical structures, which are attracting the attention of many chemists,[24,25] are potentially useful supramolecules for fluorescence color or/and intensity modulation.

II. Crystal Fluorescence Color Changes by External Stimulations. In the solid state, $[Zn_2\mathbf{L^1}_2]$ displayed other interesting optical properties. Under irradiation with a convenient UV lamp ($\lambda = 365$ nm), $[Zn_2\mathbf{L^1}_2]$ crystals emitted a bluish-green fluorescence; however, this fluorescence changed to a light blue after we ground the crystal. Both fluorescence microscopy (Figure 4a,b) and the fluorescence spectra (Figure 5) confirmed the change. The emission maximum wavelength of the crystals of $[Zn_2\mathbf{L^1}_2]$ was 488 nm, and that of the crushed powder was 474 nm, while the emission maximum wavelength of $[Zn\mathbf{L^2}_2]$ was 440 nm. The single-crystal fluorescence lifetimes (Table 1) were 1.04 ns ($[Zn_2\mathbf{L^1}_2]$) and 6.16 ns ($[Zn\mathbf{L^2}_2]$). After grinding, the lifetime of $[Zn_2\mathbf{L^1}_2]$ became longer (3.17 ns). As compared to Figure 5, the length of lifetime completely corresponds to the emission wavelength. On the analogy of the lifetime data in solution, we can suppose that lifetime and $\pi-\pi$ interaction of the chromophore are correlated. Thus, it was likely that the crush of $[Zn_2\mathbf{L^1}_2]$ crystal induced a decrease of the $\pi-\pi$ interaction.

Other external stimulations generated similar fluorescence changes. When $[Zn_2\mathbf{L^1}_2]$ crystals were set in a THF vapor-saturated vial at 20 °C for 18 h, the fluorescence color changed to a light blue. The fluorescence microscopic image appears in Figure 4c. The shade of the fluorescence color was almost the same as that of the crushed powder.

When single crystals of $[Zn_2\mathbf{L^1}_2]$ were heated in vacuo, a little sublimation took place. We then tried to sublime these crystals under a fluorescence microscope. When the crystals were heated under N_2 gas, two kinds of crystals, which were green- or blue-fluorescent microcrystals, were deposited on the cover glass (Figure 4d). These two colors resembled the fluorescence colors of the $[Zn_2\mathbf{L^1}_2]$ crystals before and after

(24) Piguet, C.; Bernardinelli, G.; Hopfgartner, G. *Chem. Rev.* **1997**, *97*, 2005−2062.
(25) Albrecht, M. *Chem. Rev.* **2001**, *101*, 3457−3497.

Table 2. Crystallographic and Experimental Data for [$Zn_2L^1_2$], [$Zn_2L^1_2$]·THF, [$Zn_2L^1_2$]·MeOH, and [ZnL^2_2]

	[$Zn_2L^1_2$][a]	[$Zn_2L^1_2$]·THF	[$Zn_2L^1_2$]·MeOH	[ZnL^2_2][a]
formula	$C_{48}H_{60}N_4O_4Zn_2$	$C_{52}H_{68}N_4O_5Zn_2$	$C_{49}H_{64}N_4O_5Zn_2$	$C_{24}H_{32}N_2O_2Zn$
a, Å	11.3432(3)	15.307(6)	12.50(2)	13.7768(5)
b, Å	16.2924(3)	19.782(6)	14.17(1)	12.8301(5)
c, Å	24.2065(6)	16.817(7)	15.80(2)	14.3768(6)
α, deg	90	90	62.01(9)	90
β, deg	90.9037(5)	99.73(4)	82.3(1)	111.446(2)
γ, deg	90	90	76.7(1)	90
Z	4	4	2	4
V, Å^3	4510.0(2)	5019.0(3)	2405.1(5)	2364.3(2)
D_{calc}, g cm^{-3}	1.307	1.270	1.270	1.253
crystal system	monoclinic	monoclinic	triclinic	monoclinic
space group	$P2_1/n$ (No. 14)	$P2_1/c$ (No. 14)	$P\bar{1}$ (No. 2)	$P2_1/n$ (No. 14)
crystal size, mm	0.45 × 0.35 × 0.30	0.40 × 0.35 × 0.25	0.60 × 0.40 × 0.20	0.50 × 0.25 × 0.12
color, habit	yellow, prism	yellow, prism	yellow, plate	colorless, prism
fluorescence	green	green	light blue	blue
$2\theta_{max}$, deg	55.0	54.8	55.0	55.0
no. measured reflections	40713	47374	20606	23471
no. independent reflections	10256 [R_{int} = 0.055]	11357 [R_{int} = 0.055]	10196 [R_{int} = 0.064]	5383 [R_{int} = 0.045]
μ, mm^{-1}	1.110	1.005	1.045	1.059
no. reflections observed[b]	6954	7336	6406	3752
no. parameters	523	637	609	262
R[c]	0.0365	0.0490	0.0760	0.0380
R_W[d]	0.0853	0.1010	0.1850	0.0670
GOF	1.156	0.811	1.142	1.573

[a] Structure determination of these complexes was briefly reported in ref 12. [b] $I > 1.5\sigma(I)$. [c] $R = \sum||F_o| - |F_c||/\sum|F_o|$. [d] $R_w = [\sum w(F_o^2 - F_c^2)^2/\sum w(F_o^2)^2]^{1/2}$.

Table 3. Selected Bond Lengths (Å) and Angles (deg) in [$Zn_2L^1_2$], [$Zn_2L^1_2$]·THF, [$Zn_2L^1_2$]·MeOH, and [ZnL^2_2]

	[$Zn_2L^1_2$]	[$Zn_2L^1_2$]·THF	[$Zn_2L^1_2$]·MeOH	[ZnL^2_2]
N1−Zn1	2.000(2)	1.985(4)	1.992(9)	1.988(2)
N2−Zn2	2.001(3)	1.998(3)	1.992(7)	
N3−Zn1	2.000(3)	1.995(3)	2.009(7)	1.997(2)[a]
N4−Zn2	1.995(2)	2.010(3)	1.995(7)	
O1−Zn1	1.912(2)	1.896(3)	1.900(6)	1.905(2)
O2−Zn2	1.902(2)	1.900(3)	1.907(7)	
O3−Zn1	1.902(2)	1.920(3)	1.893(7)	1.921(2)[b]
O4−Zn2	1.911(2)	1.902(3)	1.916(7)	
N1−Zn1−N3	119.60(10)	125.49(14)	119.4(3)	116.97(10)[a]
N1−Zn1−O1	96.21(9)	96.37(14)	96.8(3)	96.41(8)
N1−Zn1−O3	115.99(10)	102.73(14)	121.8(3)	108.29(9)[b]
N3−Zn1−O1	108.83(9)	120.96(12)	103.4(3)	119.43(9)[a]
N3−Zn1−O3	96.76(9)	94.99(12)	96.1(3)	94.62(8)[a,b]
O1−Zn1−O3	120.91(9)	116.10(12)	119.4(3)	122.20(8)[b]
N2−Zn2−N4	124.9(1)	119.84(14)	121.6(3)	
N2−Zn2−O2	96.95(9)	95.12(13)	97.2(3)	
N2−Zn2−O4	106.54(10)	110.51(13)	117.5(3)	
N4−Zn2−O2	116.46(10)	117.52(12)	109.2(3)	
N4−Zn2−O4	95.72(10)	94.82(12)	93.8(3)	
O2−Zn2−O4	117.36(9)	120.76(12)	119.1(3)	
N1−C1−C2−N2	72.0(4)	64.9(5)	71.7 (1)	
N3−C3−C4−N4	66.5(3)	68.4(2)	59.1(9)	

[a] N3 should be replaced by N2. [b] O3 should be replaced by O2.

external stimulations. As sublimation often produces crystal polymorphism, we considered that the externally stimulated fluorescence color changes of the [$Zn_2L^1_2$] crystal originated from the crystal phase transition from a green-fluorescent crystal polymorph to a light blue-fluorescent polymorph.

The X-ray powder diffraction (XRPD) experiment yielded direct evidence about the phase transition of the [$Zn_2L^1_2$] crystals. Figure 6 depicts a plot of the experimental (+) and simulated (bold lines) XRPD patterns of [$Zn_2L^1_2$]. The former gives the structural information of the crushed [$Zn_2L^1_2$], and the latter gives that of the single crystal. It is obvious that the two diffraction patterns are not equivalent. For example, a new peak appears at $2\theta = 5.89$ ($d = 14.99$ Å) in the experimental XRPD pattern, a result which is not found in the simulated XRPD pattern of the single-crystal structure of [$Zn_2L^1_2$]. The *d* spacing values for both of these patterns are listed in the Supporting Information.

Earlier, we described the fluorescence color changes of [$Zn_2L^1_2$] brought about by various external stimulations. Probably, the external stimulations caused a phase transition of the [$Zn_2L^1_2$] crystals. Yet the question remains: what kinds of changes occurred in the crystal structure of [$Zn_2L^1_2$] after these stimulations? From the lifetime data, we can suppose that external stimulations induce a decrease of $\pi-\pi$ interaction. In the next section, we discuss the origin of the fluorescence color change by comparing the fluorescence

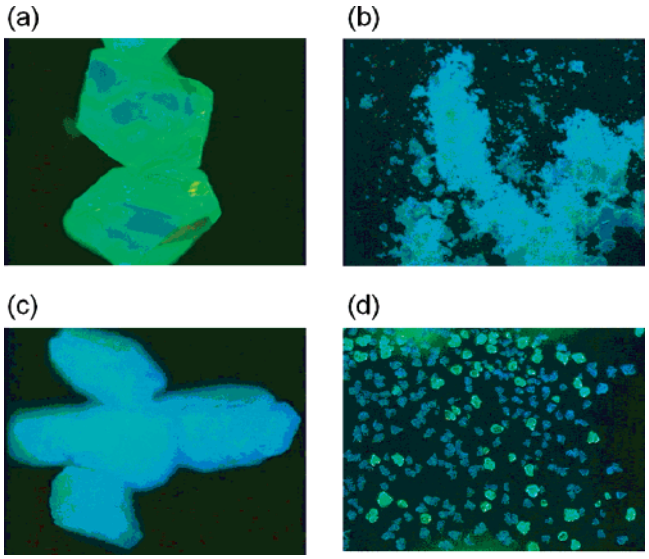

Figure 4. Fluorescence microscope images of (a) single crystals, (b) crushed crystals (powder), (c) single crystals after exposure of THF vapor, and (d) sublimed microcrystals of [$Zn_2\mathbf{L}^1_2$].

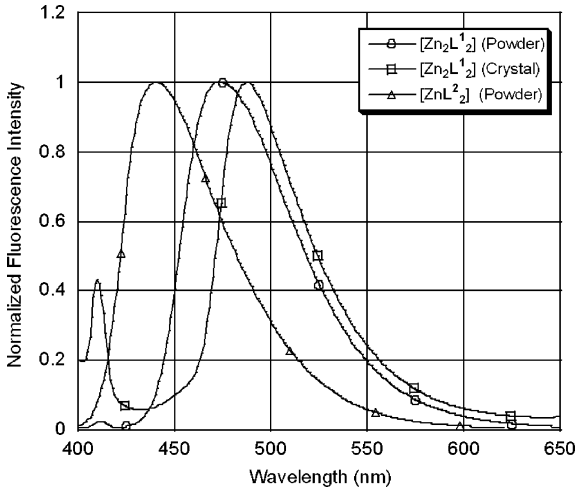

Figure 5. Solid fluorescence spectra of [$Zn_2\mathbf{L}^1_2$] and [$Zn\mathbf{L}^2_2$].

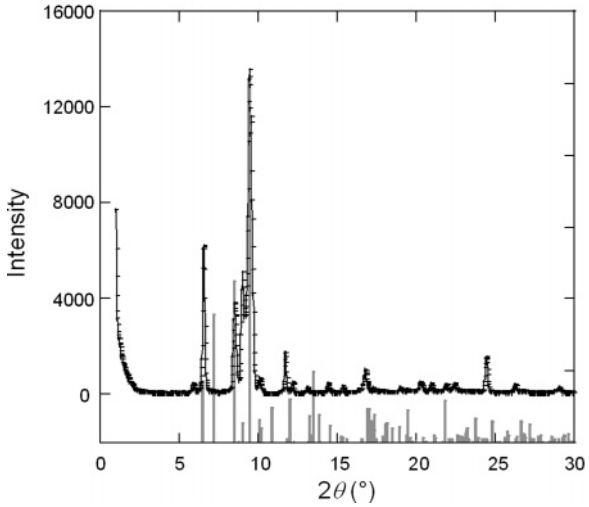

Figure 6. Experimental (+) and simulated (no symbol) powder X-ray diffraction pattern of [$Zn_2\mathbf{L}^1_2$].

properties and the crystal structures of several complexes obtained by X-ray single-crystal structure analyses.

III. Correlation between the Crystal Structures and Solid Fluorescence Properties. We believe that the solid

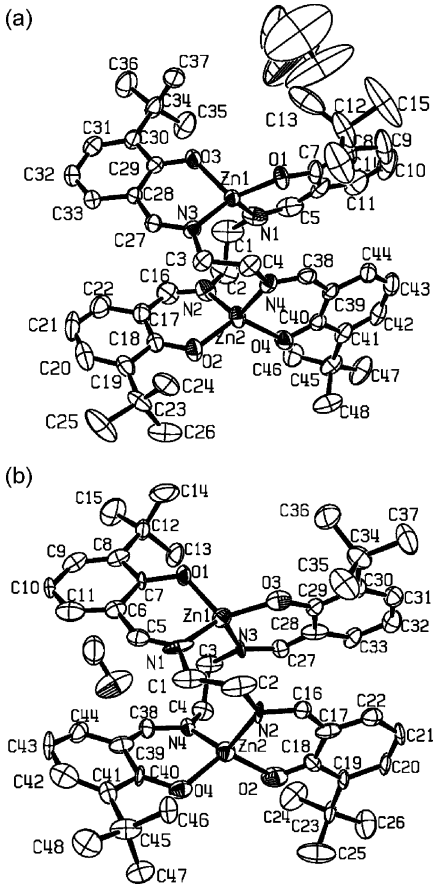

Figure 7. ORTEP drawings of (a) [$Zn_2\mathbf{L}^1_2$]·THF and (b) [$Zn_2\mathbf{L}^1_2$]·MeOH. Thermal ellipsoids for the non-hydrogen atoms were drawn at 50%. Hydrogen atoms were omitted for clarity.

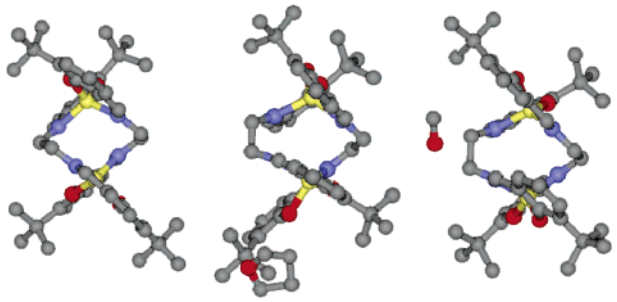

Figure 8. Comparison of crystal structures of [$Zn_2\mathbf{L}^1_2$] (left), [$Zn_2\mathbf{L}^1_2$]·THF (middle), and [$Zn_2\mathbf{L}^1_2$]·MeOH (right).

fluorescence color changes of [$Zn_2\mathbf{L}^1_2$] under external stimulation were strongly related to the packing structure. A clarification of the crystal structure of the powdered [$Zn_2\mathbf{L}^1_2$] directly from the XRPD pattern would have improved the analysis. However, although superior methods for crystal structure determination from XRPD data are now under rapid development,[26,27] we were not able to accomplish this goal for uncertainty in the unit cell.

Next, we tried to generate single crystals of [$Zn_2\mathbf{L}^1_2$] with different crystal lattices. Initially, we obtained a single crystal from THF/acetonitrile (=1/9, v/v). An X-ray crystallographic analysis showed that this crystal was a THF-solvated [$Zn_2\mathbf{L}^1_2$] ([$Zn_2\mathbf{L}^1_2$]·THF) complex. This crystal had a green fluores-

(26) Pagola, S.; Stephens, P. W.; Bohle, D. S.; Kosar, A. D.; Madsen, S. K. *Nature* **2000**, *404*, 307−310.
(27) Harris, K. D. M. *Cryst. Growth Des.* **2003**, *3*, 887−895.

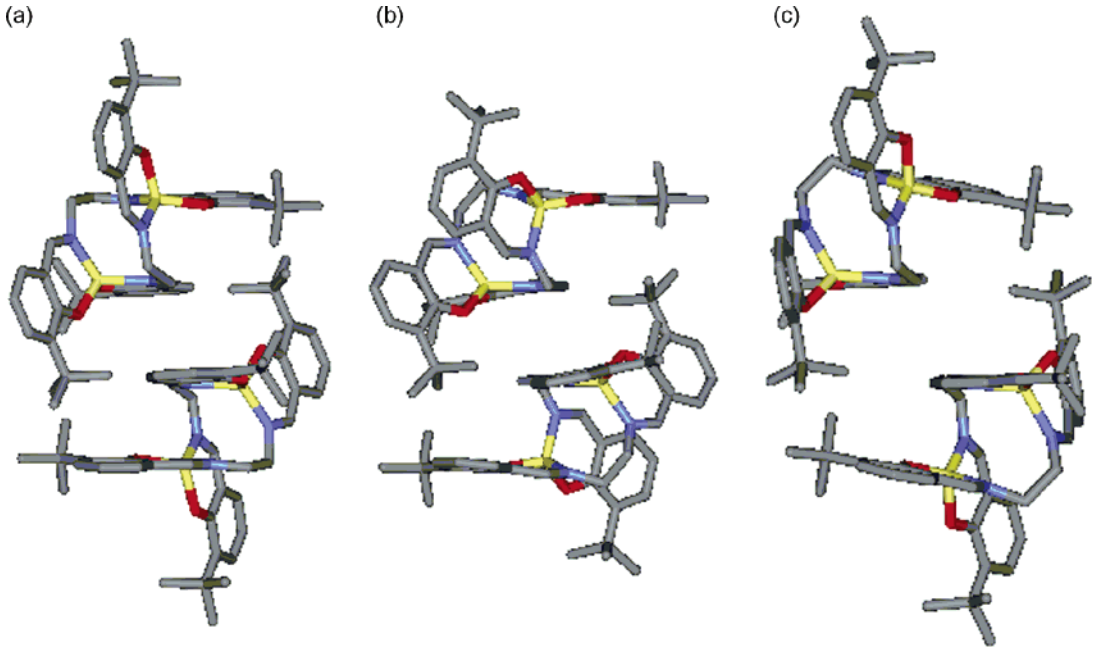

Figure 9. Crystal structures of proximate two molecules in (a) $[Zn_2\mathbf{L^1}_2]$, (b) $[Zn_2\mathbf{L^1}_2]$·THF, and (c) $[Zn_2\mathbf{L^1}_2]$·MeOH.

cence, and no recrystallization method yielded a single crystal with a blue fluorescence. We then tried to slow the diffusion complexation of three components, zinc(II) acetate dihydrate, 3-*tert*-butylsalicylaldehyde, and ethylenediamine (1:2:1), by mixing without stirring in absolute methanol at room temperature. Some precipitates appeared after several days, and although most of them were microcrystals, at last, we found a large, blue-fluorescent single crystal. By an X-ray crystal structure analysis, we discovered that this was a crystal of a MeOH-solvated $[Zn_2\mathbf{L^1}_2]$ ($[Zn_2\mathbf{L^1}_2]$·MeOH) complex. The packing structure of this complex was not equivalent to that of the powder $[Zn_2\mathbf{L^1}_2]$ after the crystal phase transition. However, because the fluorescence color of the $[Zn_2\mathbf{L^1}_2]$·MeOH was light blue, a comparison of the crystal packing structures of the $[Zn_2\mathbf{L^1}_2]$, $[Zn_2\mathbf{L^1}_2]$·THF, and $[Zn_2\mathbf{L^1}_2]$·MeOH seemed likely to hold implications for the correlation between their crystal structures and solid fluorescence properties.

The ORTEP drawings of $[Zn_2\mathbf{L^1}_2]$·THF and $[Zn_2\mathbf{L^1}_2]$·MeOH appear in Figure 7a and b. The crystal and experimental data are listed in Table 2; the selected bond lengths and angles of the complexes needed to compare molecular structures are found in Table 3. A structural comparison of these three complexes indicates that the structure of $[Zn_2\mathbf{L^1}_2]$ (green fluorescence) is only a little different from that of the latter two complexes, $[Zn_2\mathbf{L^1}_2]$·THF (green fluorescence) and $[Zn_2\mathbf{L^1}_2]$·MeOH (light blue fluorescence) (Figure 8). This result means that a small difference in a single molecular structure does not affect the fluorescence color at all and that another factor must regulate it.

Next, we examined their crystal packing structures. The crystal packing images of $[Zn_2\mathbf{L^1}_2]$, $[Zn_2\mathbf{L^1}_2]$·THF, and $[Zn_2\mathbf{L^1}_2]$·MeOH are shown in the Supporting Information. We present the extracted images of the two closest adjacent molecules in Figure 9. The intermolecular distances between two chromophoric planes of the $[Zn_2\mathbf{L^1}_2]$ and the $[Zn_2\mathbf{L^1}_2]$·THF are apparently shorter than those of $[Zn_2\mathbf{L^1}_2]$·MeOH.

Table 4. Smallest Interatomic Distances between the Chromophores of Proximate Molecules

complex	chromophore	distance (Å)	atom−atom
$[Zn_2\mathbf{L^1}_2]$	C−C′	3.46	C28−C′33
	D−D′	3.67	C42−C′43
$[Zn_2\mathbf{L^1}_2]$·THF	C−C′	3.47	C27−C′28
	D−D′	3.56	C38−C′38
$[Zn_2\mathbf{L^1}_2]$·MeOH	B−B′	3.76	C16−C′16
	D−D′	3.69	C38−C′38

Our next step was to analyze in detail the packing interaction of the chromophores. In all three complexes, there are four crystallographically nonequivalent chromophoric units A−D in one molecule as shown in Figure 1c; we use four colors (red, yellow, green, blue) to identify each of them. Evidently, chromophores C (green) and D (blue) are located near chromophores C and D of other molecules, labeled C′ and D′, respectively. However, chromophores A and B are isolated from any chromophores of other molecules. We observed similar structural features in $[Zn_2\mathbf{L^1}_2]$·THF and $[Zn_2\mathbf{L^1}_2]$·MeOH; that is, chromophores C−C′ and D−D′ in $[Zn_2\mathbf{L^1}_2]$·THF and B−B′ and D−D′ in $[Zn_2\mathbf{L^1}_2]$·MeOH were in close proximity. In Figure 10, all intermolecular chromophoric pairs are shown. From the top views, the π−π stackings in C−C′ of $[Zn_2\mathbf{L^1}_2]$, and C−C′ and D−D′ of $[Zn_2\mathbf{L^1}_2]$·THF, are apparent. The smallest interatomic distances between a chromophore of one molecule and that of an adjacent molecule are presented in Table 4. These data confirm that more than three intermolecular π−π stackings exist. Presumably, the π−π stacking effects are very weak in the other three chromophoric pairs, because the top views show there is little overlap of these chromophores.

As demonstrated by the above results, we found a correlation between the crystal fluorescence color and the crystal packing structure. When there is at least one intermolecular π−π stacking interaction in the crystal, the crystal displays a green fluorescence. Otherwise, the fluorescence color is light blue. Both the intramolecular and the intermolecular π−π interactions in the crystals red-shifted

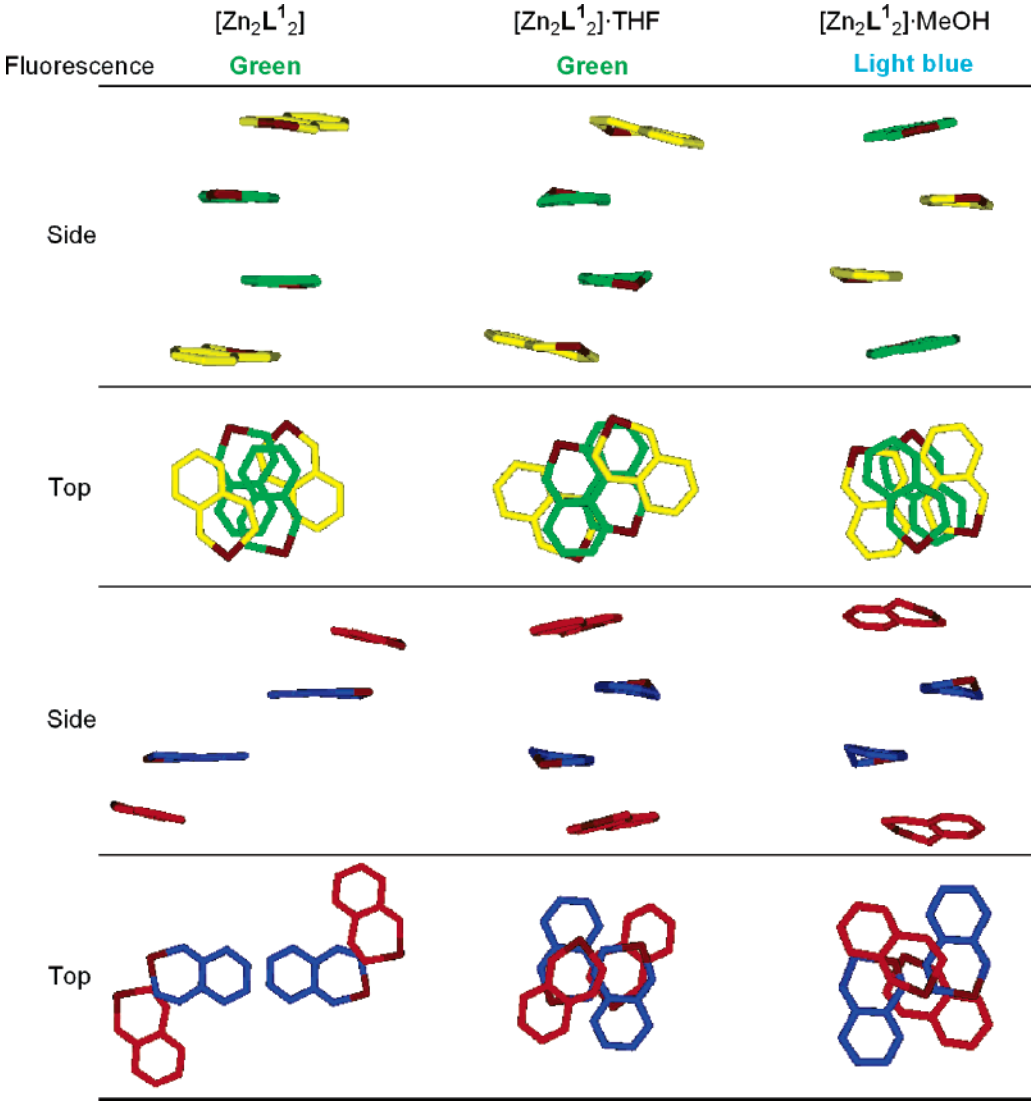

Figure 10. Top and side views of the chromophoric units in two adjacent molecules of $[Zn_2\mathbf{L}^1_2]$, $[Zn_2\mathbf{L}^1_2]$·THF, and $[Zn_2\mathbf{L}^1_2]$·MeOH. Color shows identification of the chromophoric units (red, A; yellow, B; green, C; and blue, D) and zinc atoms (brown). The chromophoric units A−D are defined in Figure 2a.

the solid fluorescence. Therefore, we conclude that the fluorescence color changes of $[Zn_2\mathbf{L}^1_2]$ under several external stimulations are the results of the crystal phase transition causing the intermolecular $\pi-\pi$ interaction to become weaker. When the intermolecular $\pi-\pi$ interaction decreases, the fluorescence lifetime must be longer. The lifetime data of $[Zn_2\mathbf{L}^1_2]$ in Table 1 completely correspond to our conclusion.

Conclusion

In this paper, we reported several interesting optical properties of a zinc(II)−salen helical complex $[Zn_2\mathbf{L}^1_2]$. In solution, an intramolecular $\pi-\pi$ interaction shifted the emission spectrum to a longer wavelength than that of a half-structured complex, $[Zn\mathbf{L}^2_2]$. In the crystalline state, an intermolecular $\pi-\pi$ interaction also took place, and this interaction regulated the solid fluorescence. If we can control the intra- and intermolecular $\pi-\pi$ interactions of fluorescent compounds with appropriate analytes, we can develop many novel fluorescent sensors. For this purpose, helical fluorescent compounds are good candidates.

Acknowledgment. We thank Drs. H. Hayakawa, M. Goto, and M. Kurahashi for helpful discussions.

Supporting Information Available: (1) X-ray crystallographic data for structural determinations of $[Zn_2\mathbf{L}^1_2]$·THF and $[Zn_2\mathbf{L}^1_2]$·MeOH (CIF); (2) packing crystal structures of $[Zn_2\mathbf{L}^1_2]$, $[Zn_2\mathbf{L}^1_2]$·THF, and $[Zn_2\mathbf{L}^1_2]$·MeOH, and (3) *d* spacing values in the XRPD patterns of $[Zn_2\mathbf{L}^1_2]$ (PDF). This material is available free of charge via the Internet at http://pubs.acs.org.

CM049744S